

A Novel High-moment Two-fluid Model for Mercury's Dynamic Magnetosphere: From the Planetary Interior to Interplanetary Space. C. F. Dong¹, L. Wang¹, A. Hakim¹, A. Bhattacharjee¹, J. A. Slavin², G. A. DiBraccio³, K. Germaschewski⁴, ¹Princeton University (C. F. Dong: dcfy@princeton.edu), ²University of Michigan, Ann Arbor, ³NASA Goddard Space Flight Center, ⁴University of New Hampshire

Introduction: Mercury's magnetosphere is highly dynamic as a consequence of its close proximity to the Sun and Mercury's weak internal magnetic field [1,2]. Compared with Earth, Mercury possesses a magnetosphere whose size is only 5% of that of the Earth, and the planet itself occupies a large fraction of the magnetosphere. In addition, the Mercury's interaction with solar wind is also complicated by Mercury's large conducting core of radius $\sim 0.8R_M$ ($R_M = 2440$ km is the Mercury's radius) [3] and the offset of its dipole center northward by $0.2 R_M$ from the equator [4]. In particular, magnetic reconnection has been frequently observed at Mercury magnetopause [5] and magnetotail [6]; the former allows direct entry of solar wind plasmas into the planetary system. The rate of reconnection in Mercury's *collisionless* magnetosphere relies on electron kinetic physics.

Method: In order to capture the kinetic behavior of Mercury's magnetosphere during the process of solar wind interaction, we investigated Mercury's magnetosphere using the Gkeyll ten-moment multifluid code that solves the continuity, momentum and pressure tensor equations of both protons and electrons, as well as the full Maxwell equations [7]. Non-ideal effects like the Hall effect, inertia, and tensorial pressures are self-consistently embedded without the need to explicitly solve a generalized Ohm's law. Previously, we have benchmarked this approach in classical test problems like the Orszag-Tang vortex and GEM reconnection challenge problem [8].

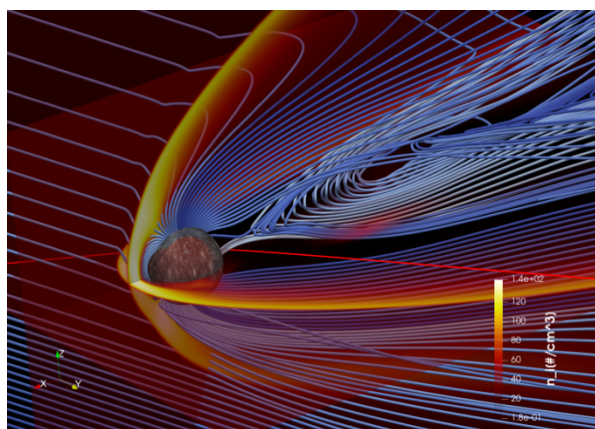


Figure 1. The three-dimensional Mercury's magnetosphere together with MESSENGER's M2 trajectory

(second flyby). The red sphere inside Mercury's surface is its conducting core $\sim 0.8 R_M$.

Results: Figure 1 shows the three-dimensional Mercury's magnetosphere based on the solar wind input from the second flyby of MESSENGER. We first validated the model by using MESSENGER magnetic field data through data-model comparisons (Figure 2).

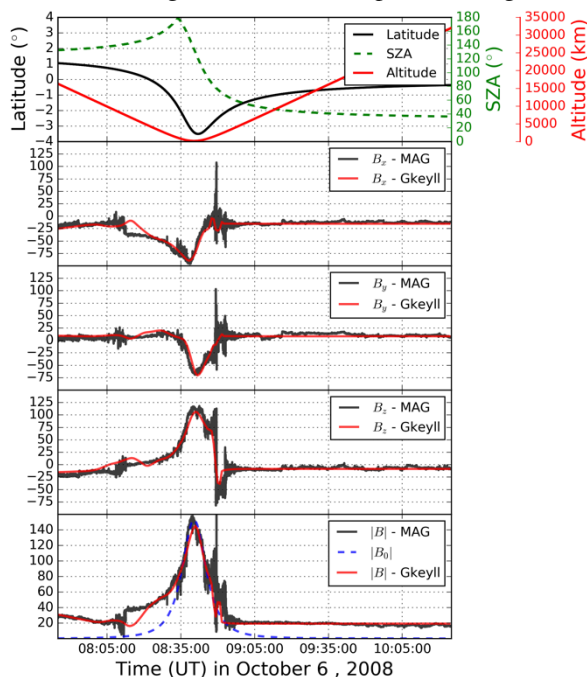


Figure 2. The data-model comparison of magnetic fields along MESSENGER's M2 trajectory.

This model is able to capture the parallel electric current in Mercury's polar region owing to its kinetic physics and, in the meantime, to reproduce the magnetotail asymmetry as observed by MESSENGER [e.g., 9,10] (Figure 3). Both day- and night-side *collisionless* magnetic reconnection are studied in detail (Figures 4 and 5). In addition, we included a mantle layer (with a resistivity profile that varies with radius) and a perfect conducting core inside the planet body to accurately represent Mercury's interior electrical property. The intrinsic dipole magnetic field may be modified by the magnetic field induced by the eddy currents on the large conducting core surface [11]. The planetary interior, therefore, is essential to capturing the correct plasma boundary locations (e.g.,

bow shock and magnetopause locations), especially during a space weather event (Figure 6).

Conclusion: We studied Mercury’s dynamic magnetosphere using a novel high-moment two-fluid model. The model is capable of reproducing MESSEGER’s observations while capturing the kinetic physics beyond a traditional magnetohydrodynamic (MHD) model. This study has the potential to enhance the science returns of both the MESSEGER mission and the upcoming BepiColombo mission (launched to Mercury in 2018).

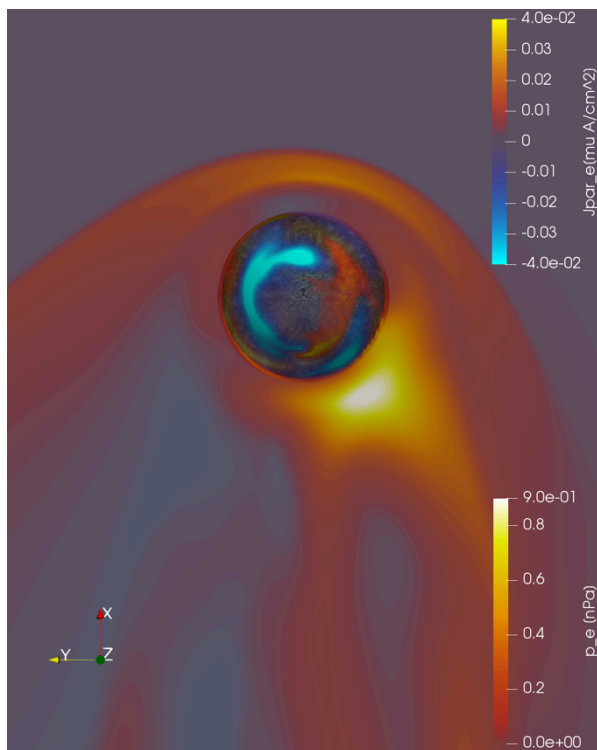


Figure 3 Parallel current in Mercury’s polar region and asymmetric electron pressure in Mercury’s magnetotail.

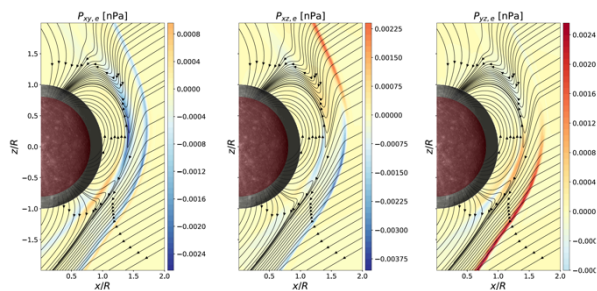


Figure 4. Magnetic reconnection at Mercury’s magnetopause. The color contour in each panel represents

the different component of electron pressure tensor off-diagonal term.

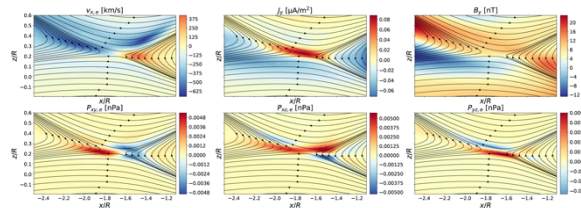


Figure 5. Magnetic reconnection at Mercury’s magnetotail. The first row shows the x-component of electron velocity, the y-component of electric current and the y-component of the magnetic field. The second row shows the difference component of the electron pressure tensor off-diagonal terms.

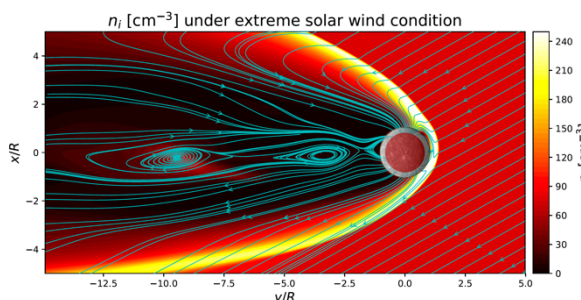


Figure 6. Mercury’s magnetosphere during an extreme space weather event. Two plasmoids are formed at Mercury’s magnetotail.

Acknowledgments: This work is supported by NSF grants AGS1338944 and AGS-1460169, and NASA grant NNX13AK31G. Resources supporting this work were provided by the NASA High-End Computing (HEC) Program through the NASA Advanced Supercomputing (NAS) Division at Ames Research Center.

References: [1] Ness N. F. et al. (1974) *Science*, 185, 151-160. [2] Slavin J. A. et al. (2007) *Space Sci Rev*, 131, 133-160. [3] Smith, D. E. et al. (2012) *Science*, 336, 214-217. [4] Anderson B. J. et al. (2011) *Science*, 333, 1859-1862. [5] Slavin J. A. et al. (2009) *Science*, 324, 606-610. [6] DiBraccio G. A. et al. (2015) *Planet. Space Sci.*, 115, 77-89. [7] Dong C. F. et al. (2017) *AGU Fall Meeting*, SM43E-03. [8] Wang L. et al. (2016) *Phys Plasmas*, 22, 012108. [9] Lindsay S. T. et al. (2016) *Planet. Space Sci.*, 125, 72-79. [10] Poh, G., et al. (2017) *J. Geophys. Res. Space Physics*, 122, 8419-8433. [11] Slavin J. A. et al. (2014) *J. Geophys. Res. Space Physics*, 119, 8087-8116.